Emissive Membrane Ion Thrusters and Their Applications

Paul J. Wilbur*, Merrill Wilson† and John D. Williams*

*Department of Mechanical Engineering
Colorado State University
Fort Collins, Colorado 80523

†Ceramatec, Inc.
Salt Lake City, Utah 84119

ABSTRACT

The mechanism of operation of a new thruster concept that utilizes solid-state ionic membranes to convert molecules into ions and transmit them to a surface from which they can be extracted into energetic beamlets thereby producing thrust is described. Results of recent experiments are used to estimate the performance of the thruster and the masses of various components required for it to perform typical satellite missions. A simple analysis is carried out over a range of specific impulses in terms of traditional mission performance parameters (thrust-to-power and total impulse-to-wet mass ratios). These results are compared to corresponding values for state-of-the-art ion and Hall thrusters. The emissive membrane thruster is shown to enable operation at 20% to 50% greater thrust-to-power ratios and 20% to 100% greater total impulse-to-wet mass ratios for a typical thrusting time. It is argued that compared to existing electric thruster designs the Emissive Membrane Ion Thruster (EMIT) will also be much less expensive and complex and that it will offer substantial improvements in scalability and reliability.

INTRODUCTION

Ion thrusters are very efficient propulsion devices that are well suited to many high specific impulse space missions. They have, however, not received widespread acceptance for military space missions because ion thruster efficiency decreases dramatically when specific impulse is reduced into the range that is optimal for many of these missions. Research is suggesting, however, that the recently proposed Emissive Membrane Ion Thruster (EMIT) can be operated efficiently in this specific impulse range[1]. This thruster concept employs the solid-state ionic conductors[2] that are becoming ever more widely used in a variety of new devices. These devices include oxygen sensors, lithium ion batteries, solid oxide fuel cells, electrochromic windows and some superconductors. They are a potentially attractive in ion thruster applications because they enable the production and delivery of ions to a surface from which they can be extracted into a beam without the complications of a plasma discharge chamber and all of its essential components.

This paper reviews the mechanism of operation of this new thruster concept and compares its mission-related performance parameters to those of other electric thrusters with which it would compete.

ESSENTIAL FEATURES OF EMIT OPERATION

Although amorphous ionic conductors exist, the typical building block of the membranes that have been tested recently[1] is a crystal like the one shown in Fig. 1. As the figure suggests, it contains propellant anions and cations connected by chemical bonds that are represented by the gray lines in Fig. 1. In order to induce a high ionic conductivity, defects are created in the crystal structure by introducing dopants and/or deviations from stoichiometry. Grain size, membrane density and purity of starting materials are also important. In an application many crystals like the one in Fig. 1 would be coupled together to form an extensive structure through which ions could be conducted at reasonable current density levels from the place where they were produced to another place where they would be extracted into beamlets. The overall sequence of events associated with ion membrane operation is shown in Fig. 2. Beginning at the right an ion is extracted from an anion pool near the downstream surface at the anode layer. As ions continue to be extracted new ones that diffuse through the ionic conductor by jumping from one vacancy site to the next replenish the anion pool. These anions are drawn ultimately from a reservoir of propellant molecules adjacent to the cathode layer shown on the left in Fig. 2. The cathode layer, which is porous and in close contact with both the propellant and the ionic conductor, and is itself a good electrical conductor, plays a very important role. It is

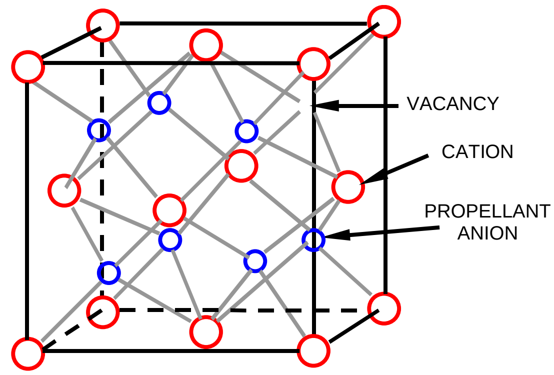

Fig. 1 Typical Binary Ionic Compound Structure

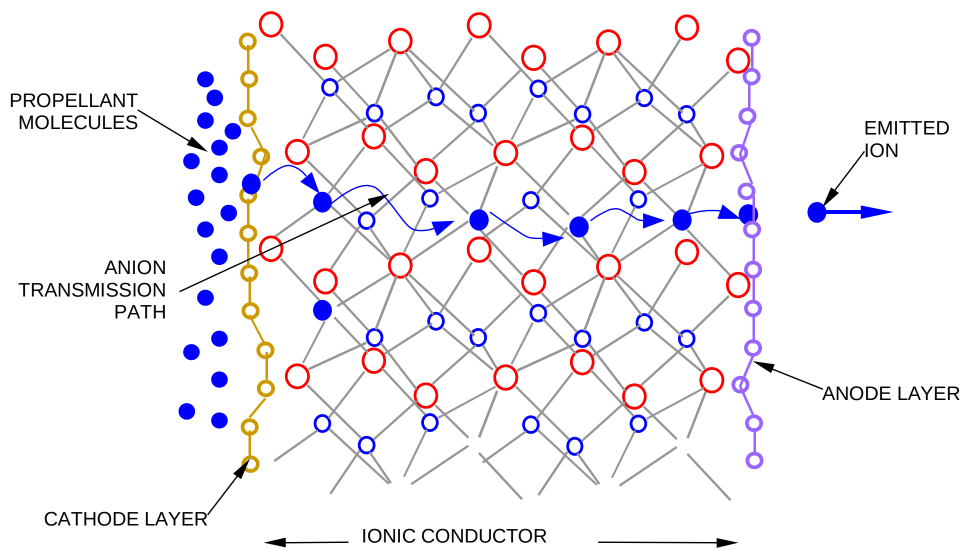

Fig. 2 Membrane Process Diagram for Anion Transmission

connected to an external current source and it thereby serves to transfer charge to propellant atoms as they pass through the layer to adjacent vacancies inside the membrane. In so doing atoms become anions and begin the process of transmission through the ionic conductor. Although the particular structure shown in Figs. 1 and 2 pertain to the flow of anions, which are negative, the process works equally well for positively charged cation transmission. In this latter case the anode layer would be on the left and the cathode layer on the right. Propellant molecules supplied to the anode layer would be stripped of an electron to form positive cations that would be conducted sequentially through the membrane. Otherwise the process of operation on positive ions would be essentially the same as that for operation on negative ions. An ion thruster specialist might envision the downstream surface of the membrane as the replacement for the screen hole plasma sheath and the membrane itself as the replacement for the entire discharge chamber plasma. Greater temperatures, applied electrical potentials, and anion/cation density gradients all facilitate the diffusion process through the ionic conductor.

The essential features of a module that might be incorporated into an array constituting an Emissive Membrane Ion Thruster are shown in Fig. 3. Its appearance is very similar to that of the cesium contact ion thrusters developed in the early 1960's.[3] Propellant supplied to the upstream side of the membrane would be ionized and transmitted to its downstream side where emission would occur under the influence of a potential applied to the accelerator electrode to attract the ions. The membrane surface would be designed and shaped[4] to focus the ions through the hole in the accelerator electrode in a way that achieves a desired effect (e.g. maximum beamlet current or minimum beamlet divergence). Because the ionization and transmission processes are surface-defined the current density of ions from this and all other emissive surfaces in the array would be uniform. This feature enables a very wide range of scalability on the levels of both the individual beamlets and the array to achieve desired thrust levels and specific impulses.

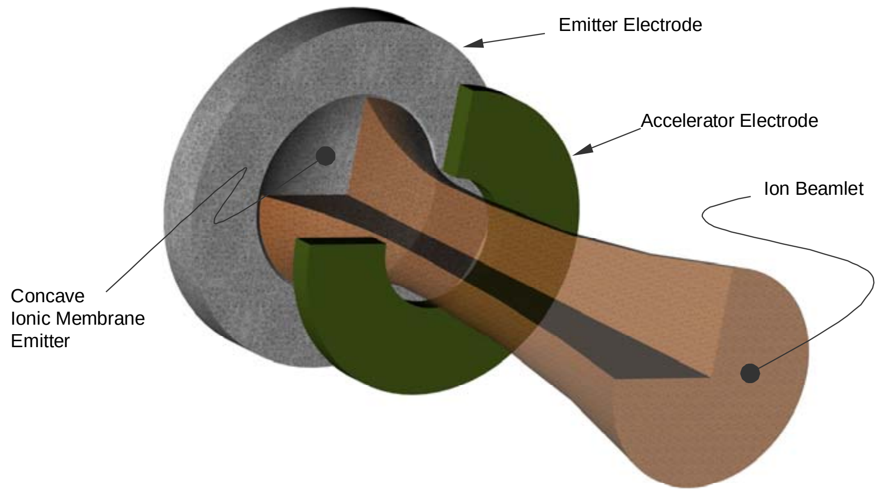

Fig. 3 The Emissive Membrane Ion Thruster Concept

As mentioned previously, good ionic conduction has been observed with many elements (e.g. silver and bismuth) from which a preferred propellant could be selected. Essentially all of those elements but oxygen produce positive ions and this desirable feature plus a preference for a heavy ion leads one away from oxygen for typical thruster applications. It is noted that the propellant can be in a gas, a liquid or even a solid. In the latter case, the solid might contact the membrane directly or a liquid might be used to transport solid particles to the membrane surface. Because the membrane is selective, only the solid particle atoms would be ionized and transported through it. In this regard it is noted that potential contaminants like the transport liquid and extraneous molecules generally do not affect the performance of ionic conductors unless they accumulate to the point where they block access to the membrane by the active element molecules.

PRELIMINARY EXPERIMENTAL AND NUMERICAL EVALUATION OF EMIT

In order to determine if the EMIT concept was viable, preliminary experiments were conducted using membranes that could be fabricated and tested using available procedures and materials[1]. Specifically, flat membranes that had been designed to ionize and transport oxygen were used. Even though these membranes used an unlikely propellant and did not focus the beamlets properly, they did enable the ionization and through-membrane transport of oxygen at ion current densities over 10 mA/cm^2 when the membrane temperature was 650°C. The current densities of oxygen ions that could actually be extracted from the downstream surfaces of the available membranes were more than an order of magnitude lower than this, but this was not unexpected because that surface of the membrane had been left in an untreated state. It is anticipated that treatment of this surface so it will have low work function for the emission of ions would enable field emission at a similar current density.

The fact that the available membranes were flat also made it impossible to conduct experiments in which high current density, well-focused beamlets were extracted. Numerical analysis was used; therefore, to demonstrate that EMIT beamlet currents would be substantially greater than those associated with conventional electron bombardment thrusters[4]. This numerical investigation was carried out over a range of specific impulses using grid dimensions scaled from those for the NSTAR thruster. Although some effort was required to obtain high-current-density, well-focused beamlets at low specific impulses it was found that this could be done even at specific impulses below 1500 sec. In particular, the analysis showed that the EMIT membrane could be shaped and positioned so a 10 mA/cm^2 focused ion beam could be extracted efficiently from it. It is argued that EMIT grid dimensions could be scaled down further so they could operate at this current density and even lower specific impulses (less than about 1000 sec).

The conduct of the experiments and the numerical analyses made it possible to compare the expected features of EMIT to those of conventional ion thrusters such as NSTAR and XIPS. This comparison indicated that EMIT should by comparison have 1) lower system cost, mass, and complexity; 2) greater system reliability and failure tolerance; and 3) higher thrust-to-power capabilities especially at low specific impulses. These system features reflect the fact that small, light, and easily manufactured EMIT membranes replace an entire discharge chamber with its magnets, hollow cathode, keeper, flow control system, and power supplies. Further, EMIT is directly scalable from multi-meter to nanometer dimensions without efficiency degradation. This makes it well suited to both micro thruster and primary propulsion applications.

ANALYTICAL MODEL DEVELOPMENT

In order to make a meaningful first-order quantitative evaluation of EMIT relative to other thruster systems, it is necessary to make comparisons in terms of mission-relevant quantities. The performance indicators selected for this study were the thrust-to-power ratio and the total impulse-to-wet mass ratio. These ratios were evaluated for two Hall thrusters (the 3-kW NASA-77M and 8-kW NASA-170M thrusters) using data from a recent comparative mission analysis study[5] and for the NSTAR ion thruster from a report that contained a breakdown of component masses[6] and from an NSTAR ground test paper[7]. The masses for these thruster systems are listed in columns 2 and 4 of Table I. Each thruster system mass ($\mathbf{m}_{ts}$) shown in Table I includes the mass of the associated propellant feed system and thruster wiring, and the power processor mass ($\mathbf{m}_{pp}$) includes the mass associated with its wiring and the Digital Control and Interface Unit. The Hall thrusters selected for this comparison don't operate over a substantial specific impulse range, so their masses were treated as constants. It was assumed that the ion thruster masses would scale with grid area and that grid hole dimensions would be adjusted so they would operate at constant current density as specific impulse was changed. This led in turn to a thruster system mass that scaled with beam current. The value of ion thruster system mass to beam current ratio (γ_{ts}) listed in column 3 for the NSTAR thruster is its mass divided by its maximum (TH15) beam current. Power processor mass was assumed to scale with power and the resultant specific masses (α_{pp}) for each thruster system are given in column 5. The solar

Table I
Thruster and Power System Masses and Specific Mass Parameters

Thruster	$\mathbf{m}_{ts}$	γ_{ts}	$\mathbf{m}_{pp}$	α_{pp}	α_{SA}	β
	(kg)	(kg/A)	(kg)	(kg/kW)	(kg/kW)	
3-kW Hall	4.9	--	9	3	10	0.1
8-kW Hall	12.2	--	28	3.5	10	0.1
NSTAR	11	6.3	18	8	10	0.1
EMIT	--	0.38	--	2	10	0.1

array specific mass (α_{SA}) and xenon propellant tankage fraction (β) values, which are listed in the last two columns, are considered typical and are the same for all of the propulsion systems considered. It is noted that xenon does not bond chemically, so it will almost certainly not be used as an EMIT propellant but it is argued that its mass will be similar to that of the propellant that will eventually be selected in future development activities. Hence, the atomic mass of xenon was used for all thruster systems in the analysis that follows.

The EMIT thruster system mass to beam current scaling factor (γ_{ts}) in Table I was based on the assumption that Laminated Object Manufacturing (LOM) could be used to fabricate the thruster as an integrated ceramic sheet from which many beamlets would be extracted. The sheet would contain (in sequence from the beam extraction side); accel grid, membrane, flow passages, and heater. It is argued that the sheet would be 1 cm thick, would be vacant over 50% of its volume, and would have a typical ceramic density of 5.75 g/cm^3. The power processor mass for EMIT is substantially less that the one for NSTAR because the only EMIT power supplies needed are those for a heater, for beam power, and to bias the accel grid. In addition, the accel supply power will operate at a very low current and, at 1500 s specific impulse, the beam supply voltage would only be 150 V.

One may now use the traditional analytical approach to estimate the performance of these various thruster systems as a function of specific impulse. In particular the total impulse-to-wet mass ratio ($\mathbf{I}_t/\mathbf{m}_o$) for constant thrust operation is assumed to be given by:

$$\frac{I_t}{m_o} = \frac{F\,t}{m_p + m_t + m_{ts} + m_{ps}} \qquad (1)$$

where **F** is the constant thrust; **t** is the total thrusting time; and $\mathbf{m}_p$, $\mathbf{m}_t$, $\mathbf{m}_{ts}$, and $\mathbf{m}_{ps}$ are the propellant, propellant tankage, thruster system, and power system masses, respectively. This equation does not include structure and payload masses because they are mission specific and their consideration could mask differences between the thruster systems.

The masses in the denominator of Eq. 1 are given by:

$$m_p = \dot{m}\,t\,, \quad m_t = \beta\, m_p\,, \quad m_{ps} = (\alpha_{pp} + \alpha_{SA})\,P = \alpha\,P \qquad (2)$$

where $\dot{\mathbf{m}}$ is the propellant flow rate and **P** is the power processor input power.

Performance data for the Hall thruster were obtained by applying the 4th order polynomial expressions given in Reference 5 that relate its mass flow rate and thrust to processor input power. Resulting values are then used to compute thrust-to-power directly. The associated specific impulse ($\mathbf{I}_{sp}$) is computed using

$$\mathbf{I_{sp}} = \frac{\mathbf{F}}{\dot{\mathbf{m}}\,\mathbf{g}} \qquad (3)$$

where **g** is the acceleration due to Earth gravity. The total impulse-to-wet mass is computed as a function of thrusting time using the mass flow rate, power and thrust in Eqs. 1 and 2.

In order to evaluate the performance of the ion thrusters, Eq. 3 is modified by relating the thrust to the ion thruster beam-ion velocity ($\mathbf{U}_b$) i.e.

$$\mathbf{F} = \dot{\mathbf{m}}\,\boldsymbol{\eta}_{\mathbf{u}}\,\mathbf{U_b} \qquad (4)$$

where η_u is the propellant utilization efficiency and the beam ion velocity is related to the net accelerating voltage ($\mathbf{V}_N$) using

$$\mathbf{V_N} = \frac{\mathbf{m_+ \, U_b^2}}{\mathbf{2\,e}}. \quad (5)$$

In this equation $\mathbf{m_+}$ is the mass of a propellant ion. The power processor input power is related to the thruster mass flow rate and beam ion velocity by the equation

$$\mathbf{P} = \frac{\mathbf{\dot{m}\,\eta_u\,U_b^2}}{\mathbf{2\,\eta_e}} \quad (6)$$

and $\boldsymbol{\eta_e}$, the electrical efficiency, is given by

$$\boldsymbol{\eta_e} = \frac{\boldsymbol{\eta_{pp}}}{\mathbf{1} + \boldsymbol{\varepsilon_B}/\mathbf{V_N}} = \frac{\boldsymbol{\eta_{pp}}}{\mathbf{1} + \frac{\mathbf{2\,e}\,\boldsymbol{\varepsilon_B}}{\mathbf{m_+}}\left(\frac{\boldsymbol{\eta_u}}{\mathbf{I_{sp}\,g}}\right)^2}. \quad (7)$$

In this equation η_{pp} is the power processor efficiency, $\boldsymbol{\varepsilon_B}$ is the beam ion energy cost, and the second expression has been obtained by substituting for $\mathbf{V}_N$ from Eq. 5. The thruster system mass scaled with the beam current $\mathbf{J}_B$ is given by

$$\mathbf{m_{ts}} = \boldsymbol{\gamma_{ts}}\,\mathbf{J_B} = \frac{\boldsymbol{\gamma_{ts}}\,\mathbf{\dot{m}\,e}\,\boldsymbol{\eta_u}}{\mathbf{m_+}} \quad (8)$$

where $\mathbf{e}$ is the electron charge and values for γ_{ts} are given in Table I. Combining Eqs. 1-6 and 8 so $\dot{\mathbf{m}}$, $\mathbf{F}$, $\mathbf{U}_b$, $\mathbf{V}_N$, $\mathbf{m}_p$, $\mathbf{m}_{ps}$, $\mathbf{m}_t$ and $\mathbf{m}_{ts}$ are eliminated and the resulting equation is simplified, one obtains the desired equation for the total impulse-to-wet mass ratio for ion thrusters.

$$\frac{\mathbf{I_t}}{\mathbf{m_o}} = \frac{\mathbf{1}}{\frac{\mathbf{1}}{\mathbf{I_{sp}\,g}}\left(\mathbf{1} + \boldsymbol{\beta} + \frac{\boldsymbol{\gamma_{ts}}\,\mathbf{e}\,\boldsymbol{\eta_u}}{\mathbf{m_+\,t}}\right) + \frac{\boldsymbol{\alpha}\,\mathbf{I_{sp}\,g}}{\mathbf{2}\,\boldsymbol{\eta_u}\,\boldsymbol{\eta_e}\,\mathbf{t}}} \quad (9)$$

The electrical efficiency that appears in Eq. 9 is obtained from Eq. 7 and the values of the other parameters that appear in the equations and have not been given are listed in Table II.

Table II
Thruster Efficiency Parameters

Thruster	ε_B	η_u	η_{pp}
	(eV/ion)	(%)	(%)
NSTAR	180*	88	95
EMIT	66**	98***	95

*At 1500-s specific impulse this value is doubled on the basis of numerical beamlet results[4] that show a high ion loss rate to the screen grid at this specific impulse.
**Value based on measurements[1] and computed radiated power losses assuming a radiative emissivity of 0.5.
*** A value of 100% is possible. This lower value reflects potential neutralizer losses.

The thrust-to-power ratio for ion thrusters obtained as the ratio of Eq. 4 to Eq. 6 becomes

$$\frac{F}{P} = \frac{2\,\eta_u\,\eta_e}{I_{sp}\,g}. \qquad (10)$$

Note that thrust-to-power is a more complicated function of specific impulse than Eq. 10 implies because electrical efficiency given by Eq. 8 is also a strong function of specific impulse.

RESULTS AND DISCUSSION

When thrust-to-power is computed as a function of specific impulse using the preceding equations and parameters, the results shown in Fig. 4 are obtained. The labeled Hall thruster

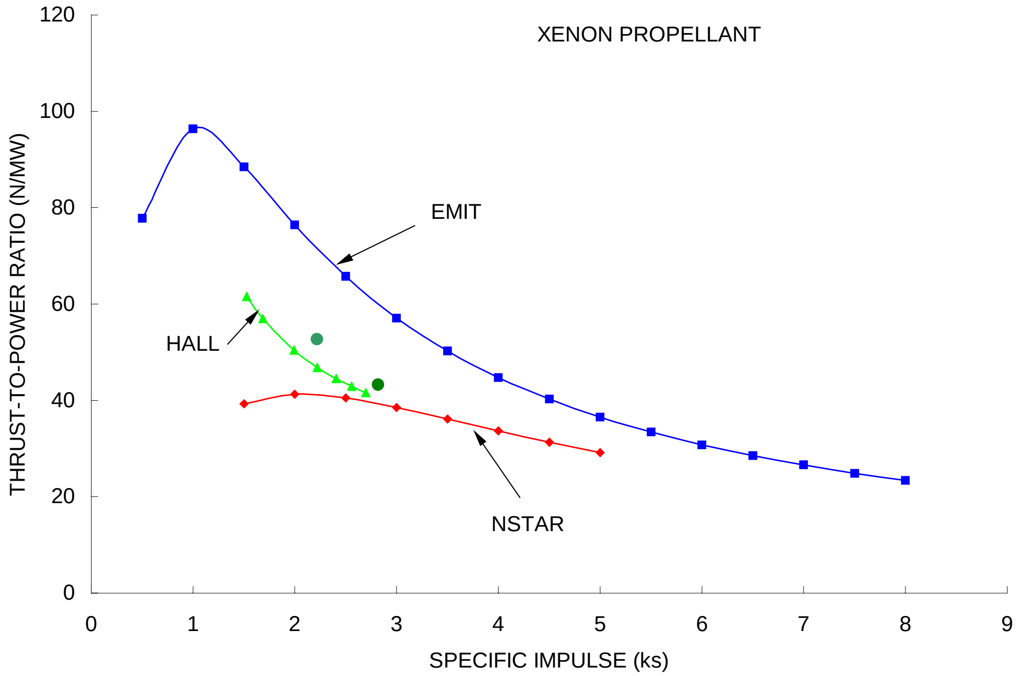

Fig. 4 Thrust-to-Power Comparison of HALL, NSTAR and EMIT Thrusters

data are those for the-3 kW unit, which did operate over the indicated range of specific impulse. The other two green, circular data points represent the performance of the 8-kW unit at two operating points (maximum power and maximum specific impulse). In each of these configurations, the 8-kW Hall thruster operated at almost constant specific impulse, so only the highest thrust-to-power points are shown. The data in Fig. 4 suggest EMIT would, over the specific impulse range investigated, operate at thrust-to-power ratios that can lie in the range 20% to 100% greater than those for the Hall and NSTAR thrusters. This would enable the EMIT to effect velocity changes proportionately more rapidly at a prescribed solar array output power.

A high value of thrust-to-power could also facilitate rapid satellite maneuvers from energy storage. If, for example, a sufficiently low-mass battery could be coupled with the low-mass EMIT array suggested here it may even become practical to perform avoidance maneuvers that could enable satellites to escape from potential hazards. This becomes possible with an EMIT array that is large enough to handle a high battery output power for a brief period of high satellite acceleration. Battery charging could be accomplished at a low charging current from a modest solar array so the solar array mass required for this function would be small. The high thrust-to-power, low thruster system mass per unit beam current of the EMIT propulsion system, and a low specific mass battery are the enabling features of such avoidance maneuvering. As shown in Fig. 4, one would want to operate near the peak in the thrust-to-mass ratio at a specific impulse of 1000 s for such avoidance maneuvering applications.

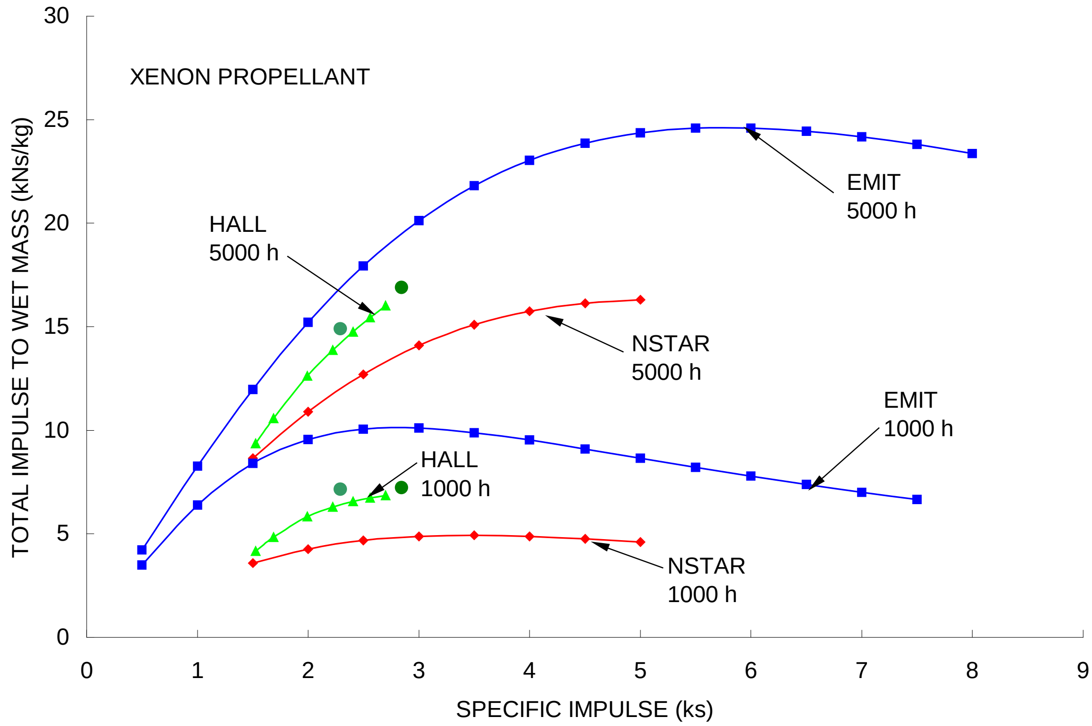

Fig. 5 Total Impulse-to-wet Mass Comparison of HALL, NSTAR and EMIT Thrusters

The effect of specific impulse on total impulse-to-wet mass is shown in Fig. 5 for the three thruster systems described in Tables I and II and the associated text. Two sets of curves, which correspond to thruster operating times of 1000 h and 5000 h are presented. The differences between these two curve sets reflect a reduction in the relative importance of the solar array, power processor, and thruster masses as they are amortized over longer thrusting times in the manner reflected in Eq. 9. Again, the circular green symbols represent data points corresponding to the 8-kW Hall thruster. The data show the EMIT exhibits total impulse-to-wet mass values over the specific impulse range investigated that are 50% to 100% greater than those for the Hall and NSTAR thrusters, respectively, for the 1000-h case. At 5000-h thrusting times, the EMIT displays performance margins that are 20% to 50% greater than those for the Hall and NSTAR thrusters, respectively. The total impulse-to-wet mass margin provided by EMIT propulsion system would be available to a designer to achieve any desired combination of (1) greater satellite lifetime, (2) greater payload mass, and/or (3) a smaller and therefore cheaper launch vehicle.

CONCLUSIONS

The Emissive Membrane Ion Thruster should be investigated further for military space propulsion applications. Preliminary evaluation of the concept suggests an EMIT propulsion system will be simple and inexpensive to build in grid scale sizes ranging from nanometer to multi-meter dimensions, that EMIT will exhibit high power and propellant utilization efficiencies over this size range, and that EMIT will be highly reliable. In addition, the thruster itself, its propellant feed system, and its power processor are all expected to have low specific masses. These features yield a thruster that is well suited for use in satellite station keeping, orbit raising, orbital maneuvering, and possibly even avoidance maneuvering missions where the optimal specific impulse is low. The extension of the ion thruster specific impulse range below 2000 s that is enabled by EMIT is expected to yield thrust-to-power ratios that are 20% to 50% greater than those for state-of-the-art Hall and ion thrusters, respectively. In addition, the low specific masses associated with EMIT appear to enable operation at total impulse-to-wet mass ratios that are 50% to 100% greater than those for these conventional thrusters over a 1000-h thrusting lifetime. Work should proceed on the selection of a preferred propellant and the development of a membrane material that can be used with it.

REFERENCES

[1] Wilbur, P. J., Wilson, M, Hutchings, K., and Williams, J. D., ***The Emissive Membrane Ion Thruster Concept*** , *29th International Electric Propulsion Conference*, Princeton, N. J., Paper IEPC-2005-164.

[2] Knauth, P. and Tuller, H.L., ***Solid State Ionics: Roots, Status, and Future Prospects***, *J. Amer. Ceramic Soc.*, Vol. 85, No. 7, 2002, pp. 1654-80.

[3] Brewer, G. R., ***Ion Propulsion***, Gordon and Breach, New York, 1970, pp.102-127.

[4] Wilbur, P. J., Farnell, C. C., and Williams, J. D., "***Ion Thruster Optical Performance Enhancement via Ion Emissive Surface Shaping"***, *29th International Electric Propulsion Conference*, Princeton, N. J., Paper IEPC-2005-95.

[5] Witzberger, K., and Manzella, D., "***Performance of Solar Electric Powered Deep Space Missions Using Hall Thruster Propulsion,"***

[6] Bond, T.A. and Christensen, J.A., "***NSTAR Ion Thrusters and Power Processors,"*** NASA/CR – 1999-209162, November 1969.

[7] Sengupta, A, Brophy, J.R., Goodfellow, K.D., "***Status of the Extended Life Test of the Deep Space 1 Flight Space Ion Engine after 30,352 hours of Operation***," Joint Propulsion Conference Paper AIAA-2003-4558, July 20-23, 2004.